ELSEVIER
CrossMark
Available online at www.sciencedirect.com
ScienceDirect
Procedia Engineering 102 (2015) 1908 – 1917
Procedia Engineering
www.elsevier.com/locate/procedia

The 7th World Congress on Particle Technology (WCPT7)

Density of laser molten polymer parts as function of powder coating process during additive manufacturing

Dietmar Drummer[a,b], Maximilian Drexler[a,b,]*, Katrin Wudy[a,b]

[a]*Collaborative Research Center 814 – Additive Manufacturing (CRC 814), Am Weichselgarten 9, 91058 Erlangen, Germany*
[b]*Institute of Polymer Technology (LKT), Am Weichselgarten 9, 91058 Erlangen, Germany*

Abstract

Mechanical and geometrical properties of parts produced by selective beam melting of thermoplastic powders depend on a large extend on interactions between following process and material parameters: Powder coating, geometry exposure and material behavior in solid and molten state. Consequently for demands of series production critical process repeatability only can be improved by fundamental studies of mentioned interactions. The following article analyzes first part density distribution for varying exposure parameters. In a second step results are correlated with typical parameters of the powder coating process during additive part generation. Furthermore part volume as well as part weight are taken into account. Result is a basic understanding of interactions between considered parameters.

Selection and peer-review under responsibility of Chinese Society of Particuology, Institute of Process Engineering, Chinese Academy of Sciences (CAS)

Keywords: Selective laser melting; heating rate; part density; coating; 3D-Printing

1. Motivation and state of the art

Formerly, techniques of additive manufacturing were used for prototype construction of special products. This actually changes, as they are now used for a vast number of new application fields by means of direct manufacturing. {Wohlers, 2011 #2993;Caulfield, 2007 #37;J.-P. Kruth, 2005 #1915}

* Maximilian Drexler. Tel.: +49-9131-8529717; Fax: +49-9131-8529709.
E-mail address: drexler@lkt.uni-erlangen.de.

Selection and peer-review under responsibility of Chinese Society of Particuology, Institute of Process Engineering, Chinese Academy of Sciences (CAS)
doi:10.1016/j.proeng.2015.01.331

Especially for technical parts, products made by additive manufacturing have grown in importance, now being much more than mere demonstration objects {Rietzel, 2008 #158;Hartmann, 2012 #2998}. Despite the huge variety of additive manufacturing processes only a few of them have the potential to meet the requirements of small series industrial manufacturing. Considering industrial requirements (e.g. reproducibility, mechanical strength) one of the most promising additive processes is the selective laser melting of semi-crystalline thermoplastic powders (Fig. 1). {Wendel, 2008 #332}

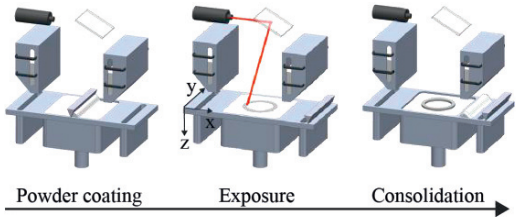

Fig. 1. Selective laser melting process (SLM) of thermoplastic polymer powder

To achieve industrial standards with beam molten thermoplastic parts basic process exploration is essential. For this purpose the sub-processes (layer coating, energy input, material consolidation) of component generation and their mutual interactions (e.g. packing density and energy input) are investigated experimentally by a specific combination of different measurement methods. Consequently selective laser sintering can be benchmarked in its entirety. Based on this basic research and built on process modeling new adapted process strategies for an improved part quality can be developed. Effects like warpage or curl should be reduced. Therefore limited process efficiency can be improved with regard to series production. {Rietzel, 2011 #3000;Rietzel, 2011 #2999}

In the following article the influence of powder coating parameters, especially coating speed and design of coating mechanism, is analyzed by using part density, which is required for mechanical part properties, as output quantity {Rietzel, 2011 #3000;Rietzel, 2010 #966}. Furthermore interaction between part density and heating rate during exposure (importance of heating rate for part structure was shown in previous investigations by the authors {Drummer, 2014 #3135;Drummer, 2013 #3130}) is taken into account. For investigations statistical design of experiments (DoE) is used. Thus, a basic understanding of the interactions between component density, powder coating process as well as exposure process is created.

2. Experimental

2.1. Laser-Melting-System (LMS)

To guarantee constant experimental boundary conditions between different experiments, it is necessary to use a special temperature stabilized and homogenized LMS. Due to a multiple heating zone system within the used LMS, the whole building chamber is nearly equally tempered. Consequently disturbing effects caused by temperature variation within the building chamber can be minimized. Moreover a laser system with nearly constant intension over whole building chamber is used (F-Theta-lenses). The scanning system is state of the art and guarantees short acceleration times as well as high precision in beam guiding. The focus diameter d_f is set to 400 µm.

According to the state of the art, layers with a thickness of d_L=100 µm are coated by an accelerated axis (here: x-axis), which is equipped with a coating tool. Actually two kinds of coating tools, according to industrial state of the art, are available: A rotating roller and a fixed blade, also called rake (Fig. 2).

Fig. 2. State of the art coating mechanisms

According to the geometry of the coating tool different powder bulk-recoater-interactions are estimated to appear. Despite the recoating tools are guided along precise NC-axis they are supposed to apply force to the powder bed. Causal for the estimated force might be powder rheological as well as technical dynamics effects. Prior investigations of the authors support this thesis {Drummer, 2012 #3036}. The element, which transmits translation energy by friction on the powder bulk is the coating mechanism. Consequently the geometrical shape of the coating mechanism is estimated to play a major role for the applied force. A force on a powder bulk results in a varying porosity of the bulk. Due to this beam absorption as well as heat transfer in the powder bulk is influenced (Fig. 3){Steinberger, 2001 #3056;Schlünder, 1988 #2178;Keller, 1998 #112}. Thus the part density is estimated to be affected.

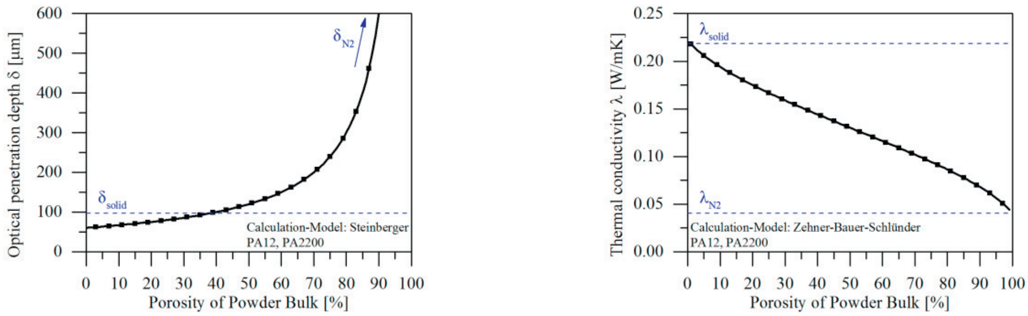

Fig. 3. Influence of powder bed's porosity on the bulk properties according to theoretical models

To consider interactions between coating process and exposure the Design of Experiments (DoE) are performed with different heating rates. As coating tools, a fixed rake and a rotating roller are considered within the DoE. Experiments are performed for different translation speeds v_t of the coating tools. The rotation speed of the roller is linear linked with the translation speed of the NC-axis over a transmission device. Moreover thermal boundary conditions in the building chamber are constant between single experiments, shown in Table 1.

2.2. Specimens

Analyses are done on two different kinds of specimens, which are designed for resolving effects on the level of a single layer and a whole part. In a prior study for investigating interaction between exposure and compaction of a powder bulk rectangular layers are exposed with a CO_2-laser (Fig. 5, left). Therefor the automatic layer coating process within the LMS is excluded. In small building chambers, shown in Fig. 4, approx. 10 g of powder are applied by hand and smoothed with a hand-rake.

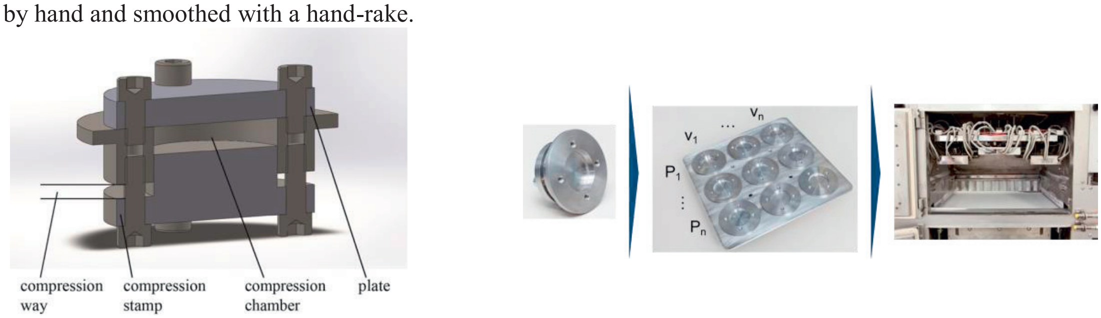

Fig. 4. Small building chamber (left); placed small building chambers in the SLM-system (right)

Additionally the powder within the building chambers can be compacted by a stamp with a defined force. Due to this fact, different forces on the bulk can be simulated by avoiding disturbing effects caused by automatic coating mechanisms. Afterwards the miniaturized building chambers are placed with in the LMS and are tempered to a building temperature of T_B=172 °C. In each building chamber a single layer is exposed with different heating rates by using the hatching exposure principal (h_s=250 µm, Fig. 5, left).

In a second experiment cubic specimens (Fig. 5, right) are built with different heating rates by using a roller as well as a rake.

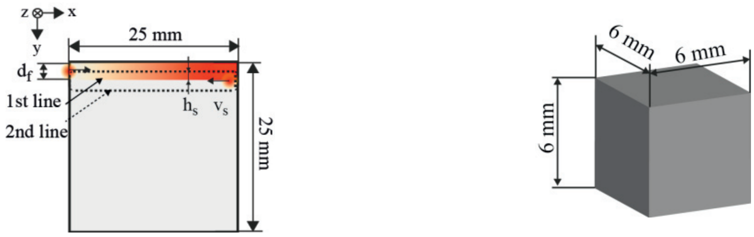

Fig. 5. Single-line-specimen (left); cube-specimen (right)

The exposure of all cubes is done with constant energy input of E=0.4 J/mm^3, according to the state of the art for processing of PA12-powder {Wegner, 2012 #3021;Wegner, 2013 #3136}. By using varying impact times t and laser powers P_L of the laser, according to {König, 1993 #209;Keller, 1998 #112;Drummer, 2014 #3135}, the heating rate H can be applied to the powder bulk.

2.3. Specimens' Analysis

Microscopy

The produced single layers are analyzed by microscopy. Therefore the rectangular layers are cut in x-z-plane. Afterwards the thickness of the layer d_d, named melting depth d_d, is measured like shown schematically in Fig. 6.

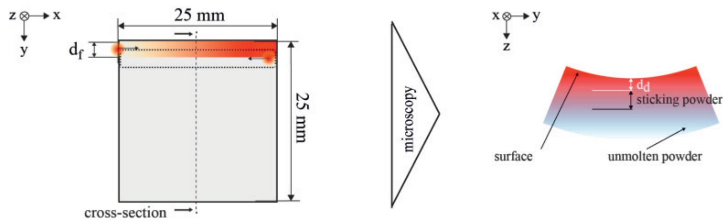

Fig. 6. Microscopic specimen analysis (schematically)

For measuring d_d the exposed specimens are cooled down in the same way and are measured after solidification. To take shrinkage and warpage in an adequate way into account absolute dimension values are not interpreted, they are only compared with specimens measured in the same way.

Density

The density of produced (and cooled down in the same way) cubic specimens is determined by a gauge (±0.001 mm) and a balance (±0.0001 g). Due to the accuracy limits, the density analysis is limited to two decimal places. Beneath the density analysis by gauge and balance computertomographic analyses are performed for some manufactured cubes. Due to the CT-pictures manual done density analysis can be controlled as well as interpreted.

2.4. Material

For done experiments a Polyamide 12 powder from EOS, Germany (type: PA2200) is used. Only new powder from the same lot number with a nearly equal particle size distribution (measured by Malvern Morphologi G3) is processed to gain equal initial conditions in each experiment. Also basic powder behavior of the used material was analyzed, like packing density and flowability (contributing to: DIN EN ISO 60 {, 2000-01-00 #2306}, DIN EN ISO 6186 {, 1998-08-00 #2305}).

Used powder for specimen building jobs has a flowability of 23.18±0.62 s, a packing density of 0.46342±0.00387 g/ml and a median particle size of $d_{3,50}$=60 µm (Fig. 7).

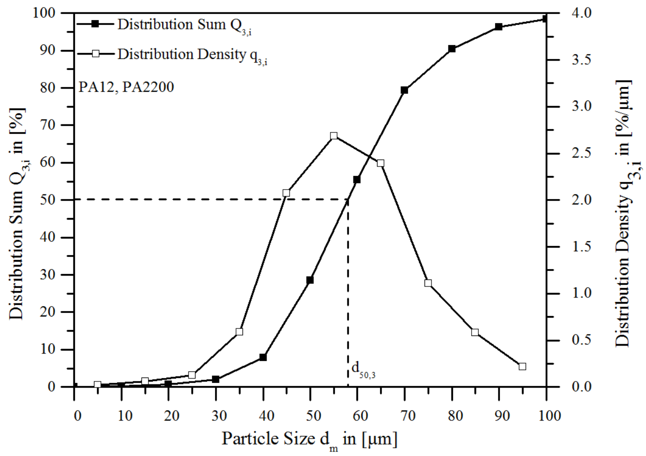

Fig. 7. Particle size distribution of used PA12-Powder

2.5. Design of Experiments (DoE)

Table 1 shows the design of experiments, which is performed once with a roller-mechanism and a second time with a rake-mechanism using cubes as specimens. The chosen values for laser power P_L, impact time t and translation speed of coating mechanism v_t are orientated next to industrial used values.

Table 1. Design of experiments (DoE)

	Process parameters (E=0.4 J/mm³)					
	Laser-Power P_L	***Heating rate H***	***Scanning speed v_s***	***Coating speed v_t***		
	[W]	***[x10⁷ K/min]***	***[mm/s]***	***[mm/s]***		
1	7.8	7.22	780	125	250	500
2	16.0	14.80	1600	125	250	500
3	22.1	20.40	2100	125	250	500
4	27.7	25.62	2770	125	250	500
5	32.9	30.40	3290	125	250	500

3. Results and discussion

3.1. Melt-Pool-Dimensions as function of bulk density

Like estimated in chapter 2.2 the bulk density of used particle bulk should affect thermal conductivity as well as optical penetration depth of a powder bulk. Consequently within compressed and un-compressed single-layers differences in layers' structure should appear. Figure 8 [11] shows the layer thickness (cross-section of a single layer) for different grades of bulk compression and heating rates as well as energy levels.

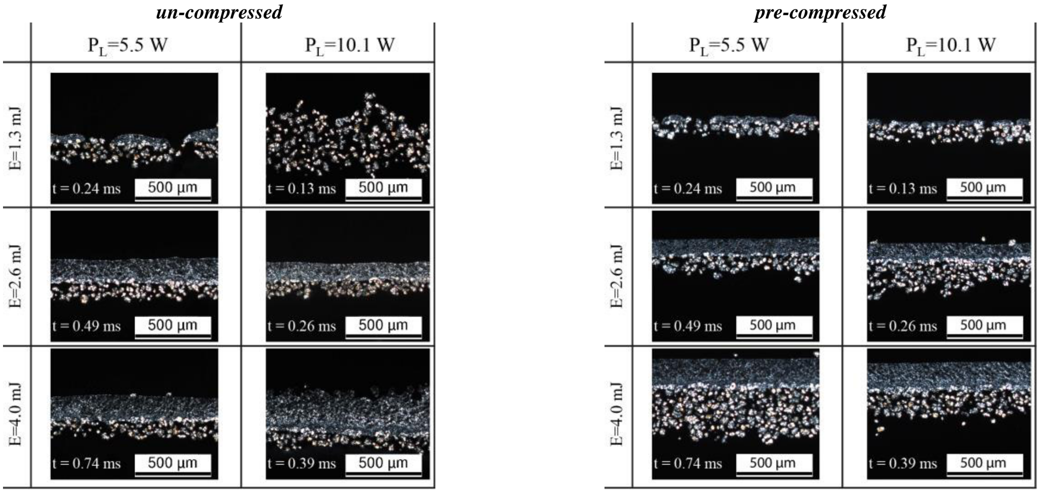

Fig. 8. Cross-section of un-/compressed single layers as function of heating rate [11]

It can be seen, that for an increasing bulk density the average thickness of a single layer lightly decreases. Furthermore a compression of the powder bulk seems to result in a denser molten layer with less defects of the melt pool. For example small energy input into uncompressed powder causes nearly no closed melting pool even on different heating rates. For pre-compressed powder even for low energy input a melt film appears. Moreover a pre-compression seems to decrease the influence of a varying heating rate on the resulting melt pool. Herein a hint can be seen, that an increased bulk density leads to changing absorption and conduction processes. Within the shown experimental setup it is not possible to resolve the appearing layer thickness whether it is caused by a reduced optical penetration depth or an enlarged thermal conduction. Furthermore the influence of the cooling process (although it was done in the same way for each layer) cannot be quantified.

3.2. Coating parameters in interaction with exposure parameters

Beneath the upon shown manual pre-compression of a powder bulk, the coating mechanism is estimated to apply a force on the powder bed during coating of a new layer. By building cubic specimens with various heating rates, coating speeds and coating tools it is analysed how on single-layer-level discovered interactions appear on part level. Especially for enlarged coating speeds and a fixed blade coating tool applied forces should be increased compared to a slow coating motion and a reverse rotating coating roller. Based on an applied force part density is estimated to vary.

Furthermore coating parameters are estimated to affect the process reproduceability due to different thermal interaction times between coating mechanisms and exposed layers. Figure 9 shows the number of finnished building jobs for various coating speeds and mechanisms.

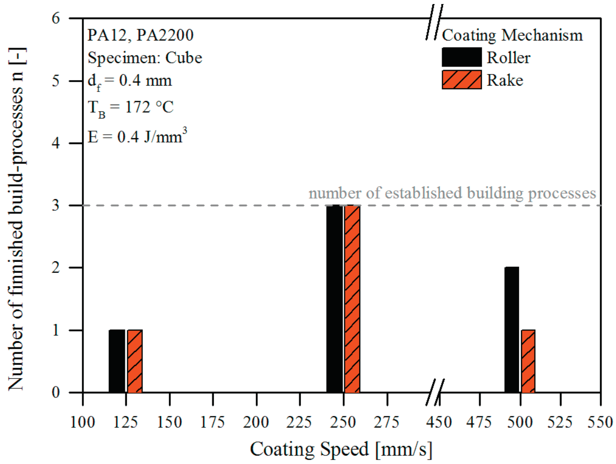

Fig. 9. Building process reproducibility as function of coating parameters

In Figure 9 it is obvious that for small as well as high coating speeds independent fromt the used mechanism the reproduceability of the building process declines. Consequently an optimal coating speed, independent from coating mechanism, seems to exist. The independency of the reproduceability of the building process from the coating tool is a hint that the interaction time between the coating mechanism and the exposed area is the dominating factor considering reproduceability. Although both coating mechanisms are estimated to apply different forces reproduceability is not affected. Consequently applied force seems not to influence warpage behavior of exposed layers. In opposite the interaction time between minor tempered coating tool and exposed area abets warpage. The interaction time is defined by the coating speed and is consequently equal for both coating tools. For coating speeds smaller than the optimal coating speed $v_{t,opt}$ the interaction time between recoater and exposed area is large enough for resulting in a significant cooling of molten area. Consequently curling based on crystallisation occurs and the warped layer is partially sticking to moving coating mechanism, which leads to process abortion. For coating speeds over $v_{t,opt}$ the fast moving recoater causes a very short interaction time. Consequently the molten areas (even for very equal tempering of the building chamber light curling appears) do not have any time for adaptation to the coating motion. Consequently the whole layer is shifted in coating direction by the recoater and the process aborts. For $v_{t,opt}$ interaction time is short enough for avoiding curling effects due to cooling of the layer and along going crystallisation. Furthermore for $v_{t,opt}$ the interaction time is long enough for giving even lightly curled layers the possibility to adapt to the coating motion. Further described interactions are shown schematically in Fig. 10.

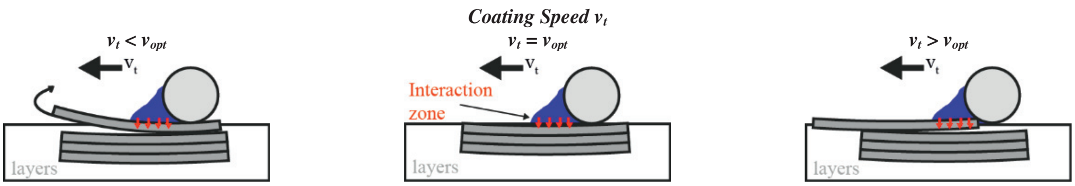

Fig. 10. Schematic interaction between coating tool and molten areas

Due to further investigations the usable window of coating speeds seems to be limited. In the following shown Figures all standard deviations are averaged over the number of successful building processes (max. 3). In each building job 5 specimens with same heating rate have been built.

Beneath process reproduceability coating speed as well as coating mechanism might affect parts' densities. Especially an applied force due to the coating process should affect parts densities as well as the interaction with exposure. Figure 11 shows the part densities for varying heating rates and different coating parameters.

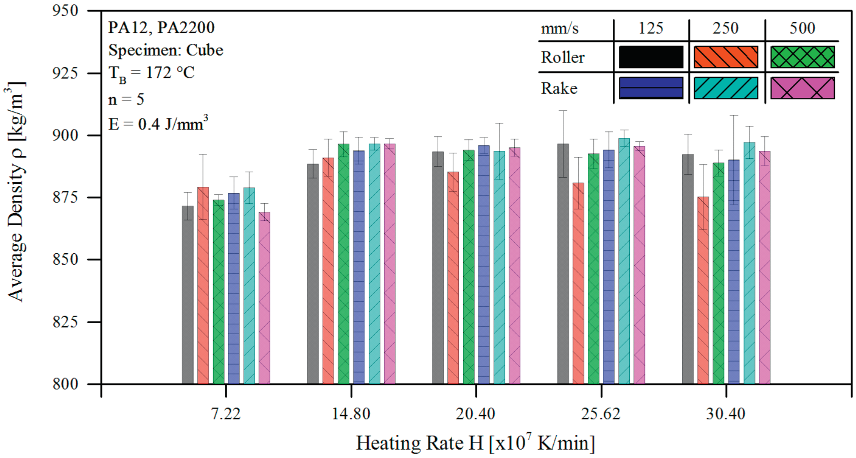

Fig. 11. Part densities as function of heating rate and coating parameters

Figure 11 illustrates, that for a slow heating with $H=7.22\cdot10^7$ K/min nearly independent from coating speeds and mechanisms the average part densities are lower than for higher heating rates. A reason for this effect might be the longer impact times of the laser at small heating rates. For a long impact time intensive thermal conduction from exposed areas into surrounding powder bed can cause an enlargement of part size. This is confirmed in Figure 14. For further increased heating rates, impact time is too short for causing significant thermal conduction into surrounding powder bed. Consequelntly for heating rates over $H=7.22\cdot10^7$ K/min average part volume should only be varied by the influence of changing coating parameters.

Considering the influence of coating speed Figure 11 shows density variations for different speeds with both coating mechanisms. The speed dependent density variations are not significant in statistical matters. But especially for the roller-mechanism density seems to be speed dependent. A reason for this effect might be the connection between rotational and translation speed within the actual experimental setup. Due to this fact the interaction between rotation and powder influences part density. For the rake-mechanism there seems to be no speed dependency. Furthermore it can be seen in Figure 11, that only for a coating speed of 250 mm/s the rake-mechanism causes higher part densitys as the roller-mechanism. A reason for this effect might be, that for low and high translations speeds the rotation gets too slow/fast for interacting with the particles. Consequently the roller works similar to a fixed rake. Based on Figure 11 it seems likely that further estimated optimal coating speed $v_{t,opt}$ exists. For coating speeds under and over $v_{t,opt}$ part density is on an nearly equal level. This effect occurs for a rake recoater as well as a roller recoating system. Thereby the rake recoater seems to abet higher part densites than the roller recoater for a coating speed of $v_t=v_{t,opt}$. This trend can be confirmed by CT-Scans, shown in Figure 12.

Fig. 12. CT-Scans for cubic specimens exposed with varying heating rates at constant coating speed

Thereby parts' density is an accumulated dimension based on the parts' volume and weight. Due to this fact volume and weight of specimens is analysed to investigate the reasons for in Figure 11 shown density variations in detail. Figure 12 shows the weight of specimens for different coating speeds, mechanisms and heating rates.

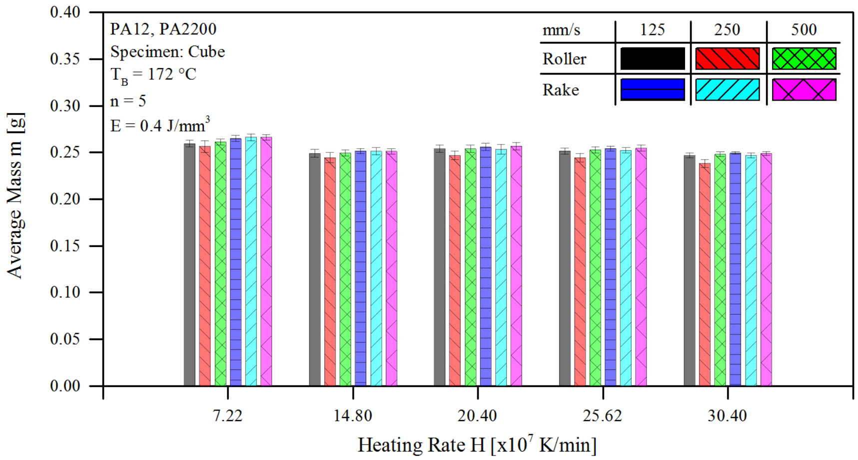

Fig. 13. Specimens' weight as function of coating speed

According to Figure 13 the weight remains nearly constant over tested parameters. Only for a low heating rate of H=7.22·10^7 K/min the part weight seems to be slightly higher. Herein another confirmation can be seen, that a size enlargement of the specimens due to impact time of the laser linked thermal conduction occurs. For the estimated optimal coating speed $v_{t,opt}$ only for the roller-mechanism part volume is increasing significantly. A reason might be, that for this coating speed the along going rotation transports more powder in a fluidisized bulk in front of the roller than it presses into the powder bed. For the rake-mechanism no changes in part weight as function of coating speed appear. Due to the minor changes in part weight the variations in part-density (Fig. 11) depend on changes in part-volume, shown in following Figure 14.

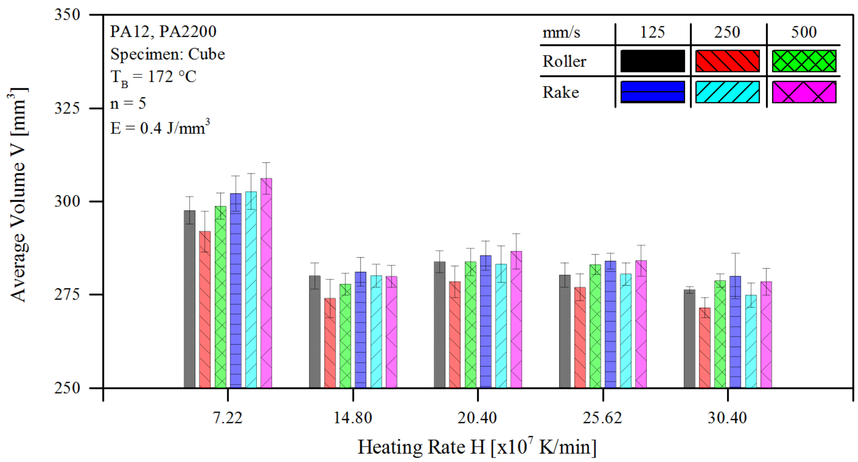

Fig. 14. Specimens' volume as function of coating speed

The part volume shows the inverse trend of parts' densities, shown in Figure 11. Especially for a heating rate of H=7.22·10^7 K/min the part volume is enlarged. This effects fits to the estimation of a size enlargement of the specimens due to thermal conduction. Furthermore for the rake-mechanism as well as for the roller-mechanism the part volume is lowered for v_t=$v_{t,opt}$. Reasonalble for this beahivour might be the interaction time between coating mecanism and prior exposed slice, like explained above. The shift of layers (Fig. 10) for high (v_t>$v_{t,opt}$) as well as minor (v_t<$v_{t,opt}$) coating speeds seems to cause higher part volumes.

4. Conclusion

Within the paper it is shown, that the density of laser motlen parts is a function of applied heating rate as well as applied coating parameters and mechanisms. Meanwhile part volume is much more sensitive against parameter changes than the part weight. Nevertheless the estimation of applied forces by the coating mechanisms can not entirely confirmed on part level although it is clearly appearing on single-layer-level. Applied forces might cause higher bulk densities and consequently changed penetration and conduction properties. Due to these changes in bulk properties molten area enlarges or decreases. Beneath volume variation caused inderict by changed bulk and along going thermal and optical properties even the cooling of produced specimens influences the later on meassured part volume. Although specimens have been cooled down in the same way changed bulk properties due to the coating process can influence appearing shrinkage behavior. Due to this fact an inline meassurement of the melt pool geometry is performed in future work of the authors to resolve effects causing volume variations. Moreover authors prepare a new experimental setup, in which the rotation of the roller system is independent from the translation movement. Consequently the understanding of powder coating process will be more detailled in future work, for enhancing reproducability and produced part properties of laser melting process.

5. Acknowledgements

The authors want to thank the German Research Foundation (DFG) for funding Collaborative Research Centre 814 (CRC 814), sub-project B03.

6. References

[1] T. WOHLERS: *Wohlers Report 2011-State of the industry.* 2011.

[2] B. CAULFIELD, P.E. MCHUGH, S. LOHFELD: Dependence of mechanical properties of polyamide components on build parameters in the SLS process. In: *Journal of Materials Processing Technology* 182 (2007), S. 477-488.

[3] B.V. J.-P. KRUTH, J. VAN VAERENBERGH, P. MERCELIS, BENCHMARKING OF DIFFERENT SLS/SLM PROCESSES AS RAPID MANUFACTURING TECHNIQUES, Int. Conf. Polymers & Moulds Innovations, Gent, Belgium, 2005.

[4] D. RIETZEL, F. KÜHNLEIN, R. FEULNER, G. HÜLDER, C. VON WILMOWSKY, C. FRUTH, E. NKENKE, E. SCHMACHTENBERG, Breaking Material Limitations in Selective Laser Sintering - An Opportunity for Medical Additive Processing, in: S.E.C.o.M. Polymers (Ed.), SPE European Conference on Medical Polymers, Belfast, UK, 2008, pp. 61-65.

[5] W. HARTMANN, T. HAUSOTTE, D. DRUMMER, K. WUDY: Anforderungen und Randbedingungen für den Einsatz optischer Messsysteme zur In-Line-Prüfung additiv gefertigter Bauteile. In: *RTejournal - Forum für Rapid Technologie* 2012 (2012).

[6] B. WENDEL, D. RIETZEL, F. KÜHNLEIN, R. FEULNER, G. HÜLDER, E. SCHMACHTENBERG: Additive Processing of Polymers. In: *Macromolecular Materials and Engineering* 293 (2008), S. 799-809.

[7] D. RIETZEL, M. DREXLER, F. KÜHNLEIN, D. DRUMMER, Influence of temperature fields on the processing of polymer powders by means of laser and mask sintering technology, Solid Freeform Fabrication (SFF), Austin, Texas, 2011, pp. 252-262.

[8] D. RIETZEL, M. DREXLER, D. DRUMMER, Grundlegende Betrachtungen zur Modellierung transienter thermischer Vorgänge beim selektiven Lasersintern von Thermoplasten, RTejournal - Forum für Rapid Technologie, Erlangen, 2011.

[9] D. RIETZEL, F. KÜHNLEIN, D. DRUMMER: Characterization of New Thermoplastics for Additive Manufacturing by Selective Laser Sintering In: *SPE Proceedings ANTEC* (2010).

[10] D. DRUMMER, M. DREXLER, K. WUDY, Resulting melt-pool-shape during selective beam melting of thermoplastics as function of energy input parameters, DDMC, Fraunhofer, Berlin, 2014.

[11] D. DRUMMER, M. DREXLER, K. WUDY, F. KÜHNLEIN, Effects of powder bulk density on the prorsity of laser molten thermoplastic parts, 29th International Conference of the Polymer Processing Society, Nuremberg, 2013.

[12] D. DRUMMER, M. DREXLER, F. KÜHNLEIN, Effects on the density distribution of SLS-parts, in: M. Schmidt, F. Vollertsen, M. Geiger (Eds.), Laser Assisted Net Shape Engineering 7 (LANE), Physics Procedia Elsevier B.V. Amsterdam, Fuerth, 2012.

[13] J. STEINBERGER: *Optimierung des Selektiven-Laser-Sinterns zur Herstellung von Feingußteilen für die Luftfahrtindustrie.* VDI-Verl.: Düsseldorf, 2001. - ISBN 3-18-357302-4

[14] E.U. SCHLÜNDER, E. TSOTSAS: *Wärmeübertragung in Festbetten, durchmischten Schüttgütern und Wirbelschichten.* Georg Thieme Verlag: Stuttgart, 1988.

[15] B. KELLER: *Rapid Prototyping: Grundlagen zum selektiven Lasersintern von Polymerpulver*. Universität Stuttgart, Institut für Kunststoffprüfung und Kunststoffkunde, Dissertation. 1998

[16] A. WEGNER, G. WITT, Correlation between Melt's Temperature during Laser Exposure and Part Properties in Laser Sintering, ICAT, 2012.

[17] A. WEGNER, C. MIELICKI, T. GRIMM, B. GRONHOFF, G. WITT, J. WORTBERG: Determination of robust material qualities and processing conditions for laser sintering of polyamide 12. In: *Polymer Engineering & Science* (2013).

[18] W. KÖNIG, W. EVERSHEIM, I. CELI, S. NÖKEN, C. ULLMANN: Rapid Prototyping - Bedarf und Potentiale. In: *VDI Zeitschrift* 135 (1993), S. S. 92 - 97.

[19] DIN EN ISO 60 - Kunststoffe - Bestimmung der scheinbaren Dichte von Formmassen, die durch einen genormten Trichter abfließen können (Schüttdichte) (ISO 60:1977); Deutsche Fassung EN ISO 60:1999, in: B.V. GmbH (Ed.), DIN EN ISO 60, 2000-01-00.

[20] DIN EN ISO 6186 - Kunststoffe - Bestimmung der Rieselfähigkeit (ISO 6186:1998); German Version EN ISO 6186:1998, in: B.V. GmbH (Ed.), DIN EN ISO 6186, 1998-08-00.